Additive Manufacturing Letters 18 (2026) 100395

Contents lists available at ScienceDirect

Additive Manufacturing Letters

journal homepage: www.elsevier.com/locate/addlet

Short Communication

End-capped polyamide 12: Impact of powder bed fusion-induced aging mechanisms

Fabian Neitzel *, Florian Nölle, Ivo Kletetzka, Hans-Joachim Schmid

Paderborn University, Particle Technology Group, Direct Manufacturing Research Center, Warburger Str. 100 33098 Paderborn, Germany

ARTICLE INFO

Keywords:
Powder bed fusion
Polyamide 12
Powder reuse
Post-condensation
Molecular weight
Process stability
Mechanical properties
Sustainability

ABSTRACT

Laser-based powder bed fusion with polymers (PBF-LB/P) of polyamide 12 (PA12) is an established industrial additive manufacturing technology, where powder reuse is essential for sustainability and reduced costs. This study evaluates PA12 powder with end-capped polymer chains to achieve an improved recycling performance, namely INFINAM® PA 6002 P (Evonik). The material underwent five consecutive processing cycles with 30 % virgin powder replenished after each cycle. Particle morphology, thermal properties, molecular weight evolution, melt flow behavior, and mechanical part performance were analyzed before and after artificial aging. Scanning electron microscopy confirmed stable particle shape and size distribution. Differential scanning calorimetry revealed only minor changes in melting and recrystallization behavior, while size-exclusion chromatography showed significantly lower post-condensation reactivity compared to PA 2200 (EOS), with a stable polydispersity index and a moderate increase in molecular weight. Melt volume rate measurements demonstrated that the initial viscosity as well as the increase upon aging were substantially lower than in PA 2200. Although elongation at break decreased by approximately 5 %, tensile strength and Young's modulus remained stable over the reuse cycles, suggesting that the material maintains structural integrity with only minor shifts in its mechanical profile. Therefore, the inherent stability suggests superior reusability compared to PA 2200, retaining consistent part quality with limited virgin powder addition. While PA 2200 in virgin state exhibits higher ductility, PA 6002 P appears to offer a good balance of strength, reusability, and process consistency. Consequently, PA 6002 P represents a viable, cost-effective, and sustainable alternative for industrial production.

Introduction

Powder bed fusion of polymers (PBF/P) is one of the most important additive manufacturing (AM) technologies for processing engineering plastics. In this process, a thin layer of powder is deposited, preheated, and locally melted by a laser in an iterative manner until the desired part is complete. The powder surrounding the part provides inherent support, eliminating the need for additional solid support structures. In general, the unsintered powder can be reused. However, especially for PA12, one of the most widely used materials in powder bed fusion, post-condensation reactions impose significant limitations [1–3].

PA12 for PBF/P applications is typically synthesized via the ring-opening polyaddition of laurolactam. In the absence of regulators that chemically block or deactivate the end groups, polymer chains with reactive open ends are formed. These end groups can undergo further condensation reactions, as observed in PBF/P-grade PA12 powders such as the frequently used PA 2200 (EOS). During processing, these materials are maintained at elevated temperatures near their melting point for several hours under a nitrogen atmosphere, resulting in relevant reaction kinetics of post-condensation. Under these conditions, increased chain mobility allows reactive chain ends to connect, forming longer polymer chains and releasing water in the process. Consequently, both the molar mass and melt viscosity of the material increase [1,4–7].

These phenomena are well known and have been extensively studied, with Stiller et al. [8] providing a comprehensive overview of the research landscape for polyamide powders. In general, post-condensation reactions and crosslinking are desirable in the finished part, as longer polymer chains and higher molar masses improve key mechanical properties such as elastic modulus, tensile strength, and elongation at break [1,9]. However, in the context of PBF/P powder recycling, these aging effects in unprocessed powder limit its reusability. Pham et al. [10] reported that, in aged PA 2200, higher melt viscosity resulting from increased molar mass can cause processing difficulties, such as reduced coalescence and a higher

* Corresponding author.
E-mail address: Fabian.Neitzel@dmrc.de (F. Neitzel).

https://doi.org/10.1016/j.addlet.2026.100395
Received 31 March 2026; Received in revised form 2 June 2026; Accepted 5 June 2026
Available online 6 June 2026

incidence of surface defects commonly referred to as the "orange peel" effect. Additionally, Chen et al. [11] showed that polycondensation occurs both in the solid and melt state, negatively affecting crystal structure, chain configuration, thermal behavior, and rheological properties. In particular, the influence of melt viscosity on mechanical properties was investigated by Alo et al. [7], Gazerro et al. [12] and Wegner et al. [13], who observed decreasing tensile strength, Young's modulus, and elongation at break with increasing viscosity. Similarly, Yao et al. [14] reported comparable reductions by manufacturing tensile specimens in three build orientations (XY, YZ, and Z) over eight cycles without adding virgin PA 2200 powder. Lastly, when powder aging progresses further due to repeated build cycles and prolonged exposure to high thermal loads, the stabilizer system, which typically consists of antioxidant additives, may become depleted. This depletion compromises the material's resistance to oxidative degradation, potentially leading to uncontrolled chain scission and reduced mechanical performance [1].

Consequently, aged powders are typically mixed with a defined proportion of virgin powder in industrial practice, often starting at 50 % [15,16]. The aim of this approach is to maintain melt viscosity at a level that allows reuse of aged powder without compromising part properties or surface quality due to post-condensation [1]. For PA 2200, a refreshing rate of 50 % virgin powder improves the viscosity, but tensile properties still decrease, as shown by Wudy et al. [17]. This limitation restricts the number of possible build cycles, resulting in the accumulation and subsequent disposal of significant quantities of unused aged powder. Given that part packing density in PBF/P is typically only 10–15 %, and considering PA12 powder prices averaging 70 € per kg, this material loss represents a substantial economic burden [11]. Such waste not only inflates production costs but also undermines process sustainability, highlighting a critical barrier to achieving resource-efficient additive manufacturing.

To overcome this limitation, recent research has explored diverse strategies ranging from chemical recycling to process optimization. On the material side, a closed-loop approach utilizing solvolysis combined with thermally induced liquid-liquid separation and precipitation has been proposed [18], while radiation spheroidization also offers a novel physical method [19]. Complementing these material reprocessing routes, process-based strategies have also emerged to mitigate defects and aging. For instance, a recent study proposed a low-temperature PBF/P method employing a semi-sintering process to minimize thermal aging [20]. Another innovative approach involves suppressing orange peel formation through pretreatment with low-power laser irradiation [21]. While these process and reprocessing innovations are valuable, they often require specialized infrastructure or complex operational adjustments. Consequently, the development of intrinsically recycling-optimized materials represents another viable pathway to sustainability.

One approach within this category is the development of recycling-optimized materials such as PA 2221 (EOS). In these systems, partial regulation of polymer chain growth enables a balance between post-condensation reactions, which improve mechanical properties, and the undesired rise in melt viscosity. This optimization, achieved through end-capping, helps to minimize the virgin powder replenishment rate while preserving process efficiency and material performance. Josupeit et al. [22,23] analyzed the aging behavior of PA 2221 and demonstrated that, at a refreshing rate of 32 %, melt viscosity, mechanical properties, and warpage remain stable, confirming its recycling capability. Beyond the ecological and economic advantages of such powders in powder bed fusion, recycling-optimized materials can be particularly beneficial for the development of filled polymers. When using non-end-capped polymers in these systems the negative effects of post-condensation are amplified, as non-melting filler particles may persist during processing and further impair coalescence. This effect was demonstrated by Kletetzka et al. [24] for glass bead- and glass fibre-filled powders, and by Roumeliotis et al. [25] for flame-retardant powders.

Although Evonik introduced the recycling-optimized PA12, PA 6002 P, within its INFINAM® product line in recent years, a fundamental understanding of its long-term aging mechanisms under realistic industrial recycling conditions remains lacking. While extensive research has confirmed the efficacy of end-capping in preventing post-condensation for PA12 in general, to the authors' best knowledge the specific recycling performance of PA 6002 P has not been characterized comprehensively beyond initial assessments in flame-retardant systems [26,27]. Consequently, it is currently unknown how the end-capped chemistry of PA 6002 P influences powder stability and part quality over extended reuse cycles compared to the thoroughly studied PA 2200. Therefore, this study aims to bridge this gap by systematically analyzing the aging behavior of PA 6002 P against the benchmark PA 2200 powder, specifically investigating the effects of PBF/P-induced aging on part properties after five consecutive build cycles with a 30 % virgin powder replenishment rate.

Materials and methods

Powder preparation and analysis

In this study, the polyamide 12 powders PA 2200 (EOS) and INFINAM® PA 6002 P (Evonik) were compared regarding their aging mechanisms during PBF/P. Particle morphology of both powders in virgin state was examined using **scanning electron microscopy** (SEM). Prior to imaging, samples were sputter-coated with a thin gold-palladium layer. SEM images were acquired using a Neon 40 instrument (Zeiss).

To investigate post-condensation behavior of both polymers in general, powders were **artificially aged** in a VT 6025 (Heraeus) vacuum oven. The samples were stored at 160°C for 24 h under a nitrogen atmosphere with less than 2 % residual oxygen. This protocol serves as a controlled simplification intended to replicate specific thermal exposure conditions relevant to PBF/P, rather than fully reproducing the complex thermal history experienced by powder in an actual build chamber.

The molecular weight distributions of virgin and aged powder samples were determined by **size exclusion chromatography** (SEC) in hexafluoroisopropanol (HFIP) as mobile phase at a flow rate of 1 mL/min. A combination of PSS PFG columns with porosities of 103 Å and 102 Å was used together with a L6200 (Merk Hitachi) HPLC pump and a refractive index detector (Shodex RI 101). The columns were kept at 40°C in a LaChrom Elite L-2350 (Hitachi) column oven. Standard calibration based on narrowly distributed PMMA standards was applied to evaluate the chromatographic results, using PSS WinGPC Software.

Particle size distribution (PSD) was measured by dynamic image analysis using a QICPIC system (Sympatec) according to ISO 13322-2. The nominal measuring range was from 1.8 to 3755 µm, allowing for the detection of particle sizes within this interval. Images are evaluated using the equivalent projected area circle method (EQPC). A RODOS dry dispersion unit was used to deagglomerate the particle collective prior to measurement.

Thermal behavior, particularly melting and crystallization temperatures and enthalpies, was characterized using **differential scanning calorimetry** (DSC). Measurements were conducted in accordance with ISO 11357-1 using a DSC 214 Polyma instrument (Netzsch). Samples with a mass of 5 ± 0.3 mg were heated from 30°C to 230°C and subsequently cooled to 30°C under a nitrogen atmosphere at a heating and cooling rate of 10 K/min.

To investigate melt viscosity, the **melt volume flow rate** (MVR) was determined using a Mflow (ZwickRoell) capillary rheometer. The test series was performed according to ISO 1133-1. The test temperature was set to 235°C and a test load of 5 kg was applied. To prevent distortion of the results due to moisture, the samples were dried in a laboratory oven at 105°C for 30 min prior to testing. The reported MVR values represent the average of at least five measurements per material.

Manufacturing and part properties

Test specimens were manufactured using INFINAM® PA 6002 P on a Eosint P396 (EOS) PBF-LB/P system equipped with a CO_2 laser. The build chamber and removal chamber temperatures were set to 179°C and 130°C, respectively. To ensure a turnkey processing experience for end users, laser parameters were applied using the proprietary default values provided by EOS for PA 2200 (PA 2200 Balance), which are not publicly disclosed. While this approach maximizes immediate usability, Leupold et al. [28] indicate that even minor variations in powder composition can significantly impact the PBF-LB/P process. Therefore, targeted parameter development remains essential to further optimize processability. The layer thickness was 120 µm, and the build height of 330 mm resulted in a build time of approximately 13 hours, excluding preheat and cooldown time. Additional specimens were fabricated beyond those used in this study, yielding a packing density of 7 %.

Consecutively five PBF/P processes were carried out using 100 % virgin powder for the first iteration as a reference. Subsequently, the aged powder was collected and sieved through a 245 µm mesh. For powder reuse, a mixture consisting of 70 % aged powder and 30 % virgin powder was prepared and blended in a rotary drum mixer for 30 min at 32 rpm. The same build layout was used for four consecutive cycles. Between each process, the powder mixture was prepared in the same manner as for the first reuse cycle.

In each build, 10 mm cubes for density measurements as well as Type 1A tensile test specimens were manufactured. The latter were fabricated in both X- and Z-direction to investigate material anisotropy. The X-direction corresponds to the coater movement direction, whereas specimens built in Z-direction were manufactured standing upright along the layer build direction.

Density measurements were carried out according to ISO 1183-1 using hydrostatic weighing with a YDK03 (Sartorius) density determination kit in ethanol and a CPA224S (Sartorius) laboratory scale. For each data point, five samples were measured. Porosity was calculated based on the measured part volume and literature density values of a pore-free component [29].

Mechanical testing was conducted on a 5569 universal testing machine (Instron) in accordance with ISO 527. Specimens were tested either in the dry as-built condition or after accelerated conditioning according to ISO 1110 in a WK3-180/70 (Weiss Technik) climate chamber at 70°C and 62 % relative humidity. Conditioned samples were acclimatized for one hour in standard climate every 24 hours and weighed until mass variation remained below 0.1 % over three consecutive days. Young's modulus was determined at a crosshead speed of 1 mm/min, while tensile strength and elongation at break were measured at 50 mm/min. For each data point, at least five specimens were tested.

Results and discussion

First, the particle morphology of both materials in the virgin state was compared. Subsequently, the powders were artificially aged to investigate the influence of post-condensation mechanisms on particle size distribution, thermal behavior, molar mass, and rheological properties. Finally, the effect of reusing PA 6002 P powder in PBF/P over five consecutive build cycles on part density and mechanical performance was evaluated.

Effects of post condensation mechanisms on powder properties

In general, particle shape can have a direct influence on properties relevant to PBF/P, such as flowability and bulk density, and thus may affect processability. Fig. 1 presents scanning electron micrographs of PA 2200 and PA 6002 P in their virgin state. Both powders exhibit predominantly globular, potato-like particle morphologies, with no significant differences in surface structure or shape observed. The characteristic particle shape is indicative of a dissolution precipitation manufacturing process, which is known to produce such specific morphologies [1].

During the PBF/P process, PA12 undergoes a combination of physical and chemical transformations that can significantly influence key powder properties, including particle morphology, thermal behavior, and melt viscosity [11,15]. For comparative purposes, the polymers investigated in this study were artificially aged to trigger post-condensation reactions occurring under typical powder bed fusion processing conditions.

As widely established, particle size distribution plays a critical role in determining powder processability [1]. Fig. 2 presents the volumetric particle size distribution of PA 2200 and PA 6002 P. Both materials exhibit a narrow, monomodal distribution with median particle diameters (D_{50}) of 59.81 µm (PA 6002 P) and 58.25 µm (PA 2200), respectively. Given that these powders are specifically designed for PBF/P applications, their particle size range falls within the typical specification of 20–80 µm, which is smaller than the standard layer thickness. Furthermore, the proportion of fine particles is low to ensure adequate powder flowability and consistent layer formation.

Analysis of the aged powder samples reveals no significant changes in the particle size distribution or median diameter compared to the virgin material. Thus, the artificial aging procedure employed in this study does not induce measurable alterations in particle size or distribution.

DSC measurements were performed on both materials in their virgin

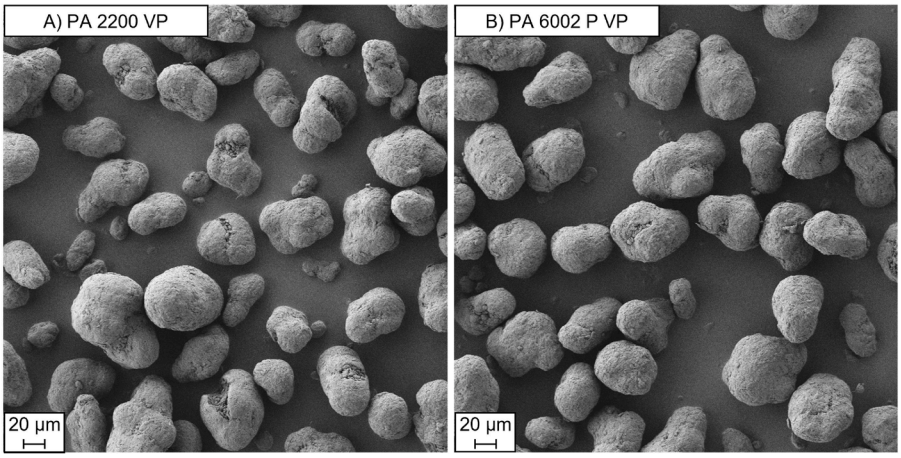

Fig. 1. SEM images of A) PA 2200 and B) PA 6002 P powder particles in virgin state (VP).

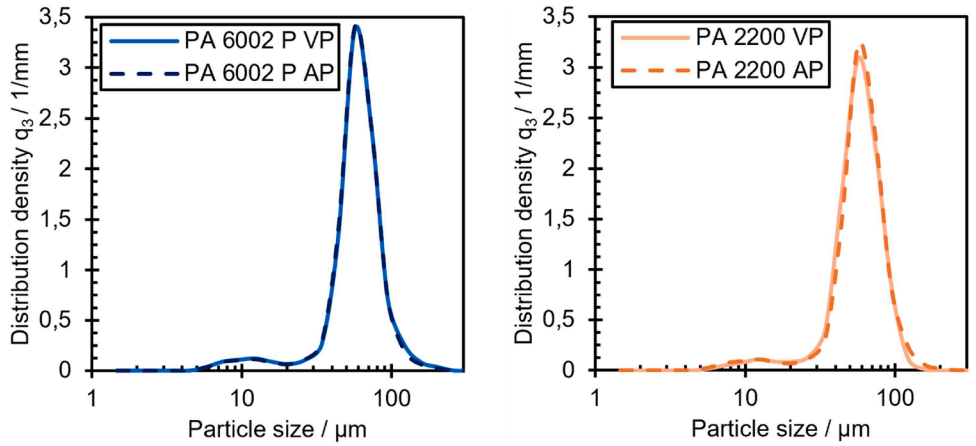

Fig. 2. Volumetric particle size distributions of PA 6002 P (left) and PA 2200 (right) in virgin state (VP) and artificially aged (AP).

and artificially aged states to investigate their thermal behavior, with particular focus on melting and crystallization characteristics. Historically, the temperature gap between the onset of melting and the onset of crystallization has been termed the 'sintering window.' However, as noted by Chatham [30], this concept is a heuristic approach that oversimplifies the complex process physics of PBF-LB/P. Consequently, this study does not treat the sintering window as a definitive processability parameter, but rather as a preliminary reference point for processing [1].

As shown in Fig. 3, the thermal behavior of both materials in the virgin state is largely comparable. Melting temperatures of 185.9°C (PA 6002 P) and 185.5°C (PA 2200), as well as recrystallization temperatures of 142.2°C (PA 6002 P) and 140.5°C (PA 2200), are typical for PBF-grade PA12. After artificial aging, both materials exhibit slightly elevated melting temperatures of 186.9°C (PA 6002 P) and 186.8°C (PA 2200), accompanied by a reduction in melting enthalpy. As reported by Chen et al. [11], the increase in melting temperature may be attributed to crystal reorganization or structural rearrangement, while the decreased enthalpy indicates a reduction in overall crystallinity. In contrast, the recrystallization behavior of both aged materials remains nearly unchanged, which is an unusual observation given that literature typically reports a decrease in crystallization onset temperature upon aging, due to reduced molecular mobility [6,31].

The post-condensation behavior of both powders can be most effectively assessed through SEC measurements or by monitoring the melt volume rate before and after artificial aging. As shown in Table 1 and Fig. 4, these SEC results reveal a significant divergence in aging behavior between the two materials.

Table 1
Molecular weight distribution parameters (Mn, Mw, Mz, Mp) and Polydispersity Index (PDI) for virgin (VP) and artificially aged (AP) PA 2200 and PA 6002 P powders, measured by SEC.

	PA 2200 VP	PA 2200 AP	PA 6002 P VP	PA 6002 P AP
Weight-average M_w / g/mol	48,759	99,269	51,196	69,910
Number-average M_n / g/mol	26,073	46,615	28,205	38,387
Polydispersity Index PDI/ -	1.87	2.13	1.815	1.821
Z-average M_z / g/mol	77,051	173,830	79,043	110,030
Peak-average M_p / g/mol	40,772	61,645	43,743	52,219

PA 2200 exhibits a significant post-condensation response to thermal aging, characterized by a 103 % increase in weight-average molecular weight (M_w) and a 125 % increase in the Z-average (M_z). This uncontrolled chain extension leads to a broadening of the molecular weight distribution (PDI increase from 1.87 to 2.13) and the formation of excessively long chains that would severely restrict melt flow.

In contrast, PA 6002 P demonstrates a controlled and moderate response. Despite undergoing the same thermal history, its M_w and M_z values increase by only 37 %, maintaining a nearly constant

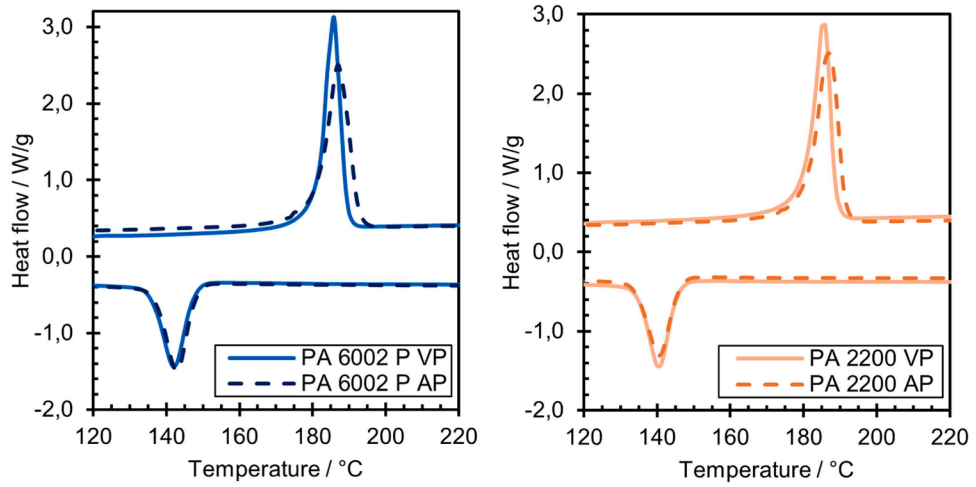

Fig. 3. DSC measurement of PA 6002 P (left) and PA 2200 (right) in virgin state (VP) and artificially aged (AP).

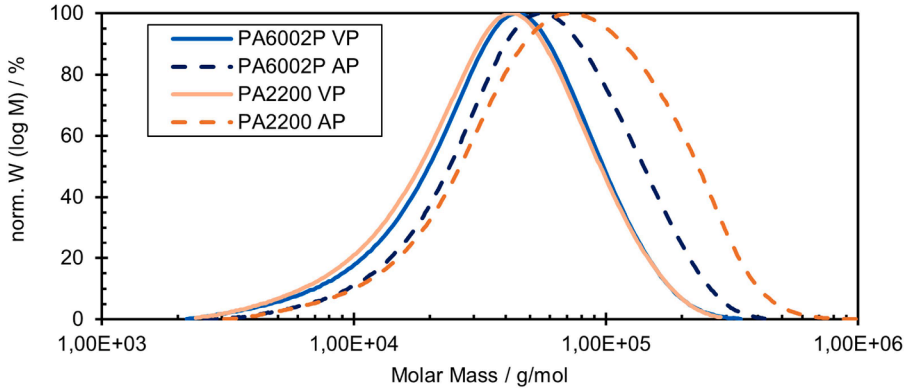

Fig. 4. Molar mass distribution of PA 6002 P and PA 2200 in virgin state (VP) and artificially aged (AP).

polydispersity (PDI 1.82). This data confirms that the end-capped architecture effectively suppresses excessive chain extension while still allowing for the beneficial chain growth that enhances mechanical properties. Consequently, PA 6002 P avoids the formation of high molecular weight fractions ($M_z > 170{,}000$) known to drive viscosity spikes and processing failures in PA 2200.

In the virgin state, PA 6002 P exhibits a significantly lower melt viscosity compared to PA 2200 (see Fig. 5). However, to further analyze this difference, additional information about the polymerization and precipitation processes would be required. Since such details are not disclosed by the manufacturer, a definitive explanation remains limited.

When comparing MVR values between virgin and aged states, a decrease in MVR was observed for both materials, indicating an increase in melt viscosity driven by chain extension via post-condensation. This rheological trend quantitatively correlates with the SEC results in Table 1, where the significant increase in number-average molecular weight (M_n) directly translates to a substantial rise in melt viscosity due to enhanced chain entanglement and flow resistance. Specifically, PA 6002 P exhibited a moderate MVR reduction of approximately 30 %, consistent with a moderate molecular weight increase, whereas PA 2200 showed a more pronounced reduction of about 63 %, reflecting a significantly higher degree of chain extension and entanglement.

Notably, the MVR of aged PA 6002 P remains higher than that of virgin PA 2200, with values of 69.22 cm^3/10 min and 60.71 cm^3/10 min, respectively. This indicates that despite undergoing post-condensation, PA 6002 P maintains a favorable flow behavior even after aging.

Based on these findings and in conjunction with the SEC data, it is concluded that the development of PA 6002 P by Evonik employs a controlled post-condensation strategy. This approach enhances mechanical properties through chain extension while keeping the reaction extent limited to avoid excessive melt viscosity increase. Consequently, this balance is assumed to enable effective powder coalescence during PBF/P, offering a pathway to high part quality even with aged material.

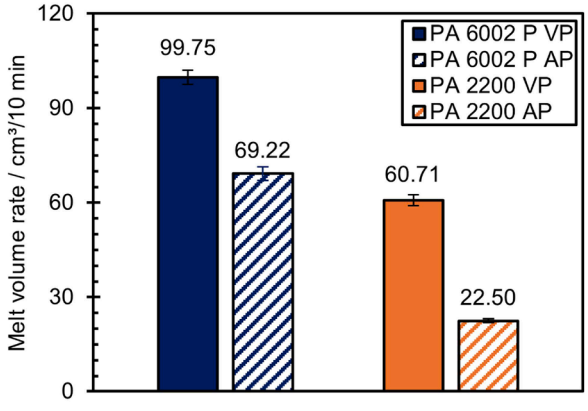

Fig. 5. Melt volume rate of PA 6002 P and PA 2200 in virgin state (VP) and artificially aged (AP).

Effects of post-condensation mechanisms on part properties of PA 6002 P

The impact of PBF/P-induced aging on part properties was evaluated over five consecutive recycling cycles, utilizing a 30 % virgin powder replenishment strategy with PA 6002 P.

Fig. 6 depicts the measured density values and the calculated porosity. Parts fabricated from 100 % virgin powder exhibit the lowest density and the highest theoretical porosity of 4.7 %. This trend is counterintuitive compared to established literature, which typically associates lower viscosity with improved fusion [31]. Crucially, the current SEC and DSC data do not support attributing this phenomenon to specific changes in chain length or crystallization kinetics. Consequently, the exact mechanism driving the higher porosity in virgin parts remains unclear and warrants further investigation.

In contrast, over the subsequent four powder reuse cycles, the porosity remained stable at approximately 3.2 %. While increasing melt viscosity in aged powders typically restricts coalescence and elevates porosity, PA 6002 P effectively maintains its densification capability throughout the process [13]. This value falls within the broad, approximate range of 3 % to 5 % typically reported for parts made from unfilled PBF-grade PA12 [1,31,32]. While this strongly implies stable coalescence, the absence of microstructural analyses limits the ability to confirm the exact state of particle fusion.

Fig. 7 presents the results of tensile tests, including tensile strength,

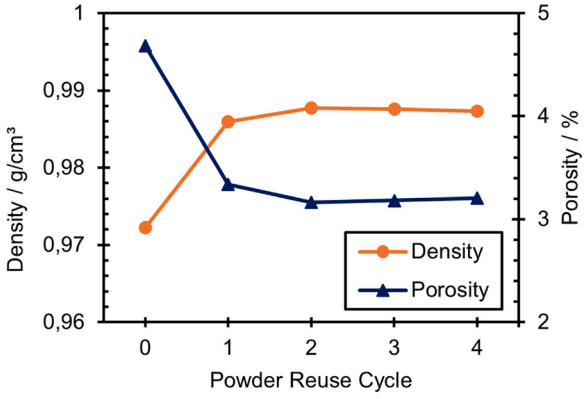

Fig. 6. Density measurement and calculated porosity of PA 6002 P: Builds 0-4 were produced sequentially via PBF/P. The first build (cycle 0) used virgin powder, while build cycles 1–4 were manufactured with a 70 % reused / 30 % virgin powder mixture. The standard deviation (±0.2) is below 1% of the measured value and therefore not visually distinguishable in the plot.

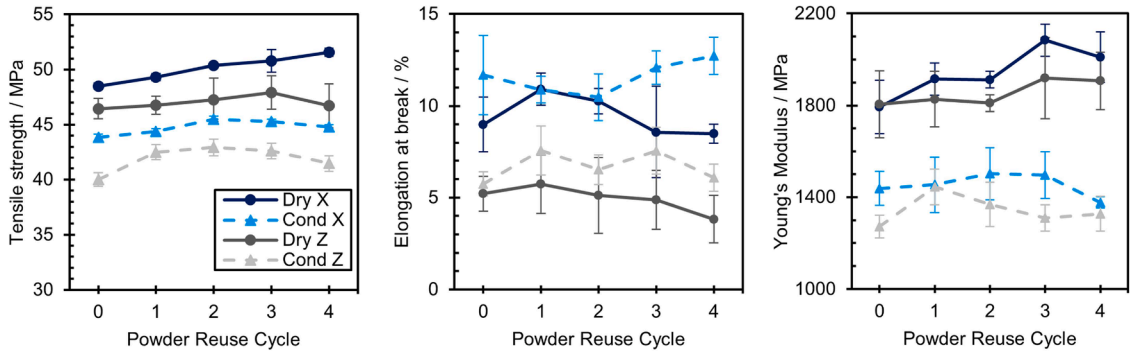

Fig. 7. Tensile test data are shown for dry and conditioned specimens manufactured with PA 6002 P in directions X and Z. Builds 0-4 were produced sequentially via PBF/P. The first build (cycle 0) used virgin powder, while build cycles 1–4 were manufactured with a 70 % reused / 30 % virgin powder mixture.

elongation at break, and Young's modulus, for specimens tested in the X- and Z-directions in dry and conditioned state. As expected, dry specimens exhibit stiffer and more brittle mechanical behavior compared to conditioned specimens. For conditioned specimens oriented in the X-direction, tensile strength is approximately 9 % lower, Young's modulus is about 25 % lower, and elongation at break is roughly 30 % higher than for their dry counterparts. This behavior is attributed to the well-known plasticizing effect of absorbed water on the polymer matrix, which enhances toughness and ductility [33].

The results also reveal the typical anisotropic behavior observed in additively manufactured parts. When parts are fabricated upright in the Z-direction, tensile strength decreases by approximately 6 % compared to X-direction specimens. However, elongation at break is significantly reduced, with a drop of up to 50 %, indicating a more pronounced loss in ductility in this orientation.

Over the course of four powder reuse cycles, most mechanical properties of the mixed powder remained stable, with no statistically significant degradation observed. While elongation at break decreased by approximately 5 %, trends toward slightly higher Young's modulus and tensile strength were noted with each processing iteration. Although these values occasionally exceeded those of the virgin powder, the magnitude of these differences falls within the range of experimental scatter. Nevertheless, the observed trend is consistent with the post-condensation-induced rise in molecular weight. The resulting longer polymer chains likely facilitate increased chain entanglement, which enhances the material's resistance to deformation and load transfer, thereby supporting the maintenance of high mechanical performance in the recycled parts.

Comparing the tensile properties of virgin PA 2200 in the dry state for both X- and Z-directions (data from EOS [16]) with virgin PA 6002 P (cycle 0, Fig. 7) reveals distinct differences. The end-capped material exhibits higher Young's modulus of 1800 MPa to 1650 MPa in X-direction, along with comparable tensile strength of approximately 48 MPa. However, the elongation at break is significantly lower at 8.9 % versus 18 %. In the Z-direction, PA 6002 P demonstrates higher tensile strength (46.45 MPa vs. 42 MPa), stiffness (1805 MPa vs. 1650 MPa), and elongation at break (5.21 % vs. 4 %) in comparison to PA 2200. Overall, virgin PA 6002 P displays a mechanical profile characterized by increased stiffness but reduced ductility, indicating a stiffer and more brittle behavior relative to PA 2200.

A review of the literature regarding the aging behavior of PA 2200, serving as an indirect benchmark, reveals a diverse range of outcomes, as part properties are highly dependent on machine settings, laser parameters, print orientation, specimen geometry, and conditioning state. Nevertheless, a trend is observed where tensile properties typically decline in correlation with decreasing part density. For instance, Wegener et al. [13] demonstrated that without virgin powder replenishment, conditioned mechanical properties decreased significantly after 100 hours of build time. Specifically, at the highest volume energy density tested, the X-direction properties showed a Young's modulus drop from 1800 MPa to 1100 MPa, tensile strength from 51.5 MPa to 29.5 MPa, and elongation at break from 15.5 % to 10.5 %. A comparable reduction was observed in the Z-direction. Similarly, Alo et al. [7] reported that after a cumulative build time of 67.72 hours, tensile strength in specimens without virgin powder replenishment fell from 40.6 MPa to 12.8 MPa. Sanders et al. [31] postulated that with a 30 % replenishment rate, tensile strength decreased from 44.5 MPa to 40.5 MPa. Most critically, Wudy et al. [17] registered severe degradation even with a 50 % virgin powder replenishment after each cycle, where tensile strength plummeted from 36 MPa to 4 MPa and elongation at break dropped from 5.5 % to 3.9 % after just 10 build cycles.

Unlike the general trend of declining properties in PA 2200 across varying refresh protocols, no significant degradation in mechanical performance is observed for PA 6002 P. This stability is evident even after multiple reuse cycles with a rather small replenishment rate of 30 % virgin powder, a condition under which Sanders et al. [31] still observed property loss in PA 2200. This consistent performance underscores the material's robust reusability and its ability to maintain high part quality under realistic recycling conditions. Consequently, PA 6002 P emerges as a viable candidate for cost-effective and sustainable industrial PBF/P processes. Its compatibility with standard laser parameters further facilitates straightforward integration into existing powder bed fusion systems, enabling immediate implementation without extensive process development.

Conclusion

The targeted investigation of PA 6002 P under PBF/P-induced aging conditions demonstrates its strong potential for sustainable additive manufacturing. The particle morphology of both virgin and aged powders remains largely unchanged, with predominantly globular, potato-like particles and a narrow, monomodal size distribution. This stability ensures consistent powder flowability and layer formation over multiple reuse cycles, which is essential for reliable process performance.

Thermal analysis via differential scanning calorimetry revealed that artificial aging induces only minor changes in the melting and recrystallization behavior of PA 6002 P. The melting temperature increases slightly, and the melting enthalpy decreases, indicating crystal reorganization and a moderate reduction in crystallinity. Importantly, the recrystallization behavior remains stable, suggesting consistent thermal response during sintering.

Size-exclusion chromatography confirmed that PA 6002 P exhibits significantly lower reactivity during post-condensation reactions compared to PA 2200. The increase in average molecular weight (M_w) is substantially smaller, and the polydispersity index remains nearly constant. This controlled molecular growth is critical for preventing excessive viscosity increases, which can compromise processability.

Melt volume rate measurements further supported these findings. While both materials show increased melt viscosity after aging, the reduction in MVR for PA 6002 P is significantly lower than for PA 2200. Notably, the MVR of aged PA 6002 P remains higher than that of virgin PA 2200, indicating superior flowability even after thermal exposure.

Mechanical testing confirmed that PA 6002 P maintained stable mechanical properties with a 30 % replenishment ratio over multiple reuse cycles with a total processing duration of 65 hours. Despite the expected increase in molecular weight due to post-condensation, tensile strength and Young's modulus remain stable over the reuse cycles. The specimens exhibited the characteristic anisotropic behavior of additively manufactured parts, with Z-direction samples showing reduced ductility and significant anisotropy in Young's modulus. However, no significant degradation in strength or toughness is detected, and mechanical performance exceeds that of virgin powder. This improvement is consistent with the beneficial effects of higher molecular mass. Compared to PA 2200, virgin PA 6002 P exhibits significantly lower elongation at break. However, it maintains consistent mechanical performance across four consecutive build cycles which highlights the material's high reusability and robustness under realistic industrial recycling conditions.

Collectively, these results indicate that PA 6002 P maintains consistent processability, thermal stability, and mechanical performance over multiple cycles, with only a marginal reduction in ductility. Its formulation leverages post-condensation reactions to enhance mechanical strength while balancing melt viscosity and ensuring consistent part quality. Quantitatively, operating with a 30 % virgin powder replenishment rate compared to the typical 50 % required for standard PA12 yields a material saving of approximately 40 % in virgin powder consumption per cycle, significantly reducing waste generation and operational costs.

Despite these observed benefits, the material has seen limited adoption in current applications. This may be attributed to its higher anisotropy compared to non-end-capped polymers, which complicates the prediction of part performance, or to the prevailing business model of PBF/P system manufacturers, which typically offer turnkey solutions with pre-optimized materials and parameters. While this approach enhances usability and lowers entry barriers for end users by minimizing the need for parameter development and providing direct technical support, it may inadvertently limit the visibility and adoption of alternative materials like PA 6002 P. Notably, the material's stable performance using standard EOS processing parameters confirms its compatibility with existing turnkey systems, suggesting its potential as a sustainable option for industrial PBF/P applications where powder reuse is a critical economic and environmental factor.

From the authors' perspective, the results provide evidence for the adoption of PA 6002 P in industrial workflows. While the demonstrated ability to sustain performance with limited virgin powder addition is promising, it remains to be determined whether even lower refreshing rates are viable. Future investigations must account for critical factors such as total process time and nesting density, as these parameters likely govern the long-term thermal history and subsequent aging kinetics in an industrial setting. This work therefore serves as a starting point for future investigations into reducing powder refreshment, with the broader aim of advancing toward near-zero waste in industrial additive manufacturing.

CRediT authorship contribution statement

Fabian Neitzel: Writing – review & editing, Writing – original draft, Visualization, Validation, Methodology, Investigation, Formal analysis, Data curation, Conceptualization. **Florian Nölle:** Writing – review & editing, Visualization, Investigation, Formal analysis, Data curation. **Ivo Kletetzka:** Investigation, Formal analysis. **Hans-Joachim Schmid:** Writing – review & editing, Supervision, Project administration, Funding acquisition.

Declaration of competing interest

The authors declare that they have no known competing financial interests or personal relationships that could have appeared to influence the work reported in this paper.

Acknowledgements

The research activities have been partially funded by Evonik Operations GmbH. The authors would like to thank Maik Grebe for his support and sharing of knowledge. The authors acknowledge support for the publication costs by the Open Access Publication Fund of Paderborn University.

Data availability

Data will be made available on request.

References

[1] M. Schmid, Laser sintering with plastics: Technology, processes, and materials, Hanser Publications; Carl Hanser Verlag, Cincinnati, Munich, 2018.
[2] A. Gebhardt, J.-S. Hötter, Additive manufacturing: 3D printing for prototyping and manufacturing, Hanser Publications; Carl Hanser Verlag, Cincinnati, Munich, 2016.
[3] J.M. Jafferson, D. Chatterjee, A review on polymeric materials in additive manufacturing, Mater. Today: Proc. 46 (2021) 1349–1365, https://doi.org/10.1016/j.matpr.2021.02.485.
[4] T.A. Osswald, E. Baur, N.S. Rudolph, Plastics handbook: The resource for plastics engineers, fifthth edition, Hanser Publications, Cincinnati Ohio, 2019.
[5] S. Koltzenburg, M. Maskos, O. Nuyken, Polymere: Synthese, Eigenschaften und Anwendungen, Springer Berlin Heidelberg, Berlin, Heidelberg, 2024.
[6] K. Wudy, D. Drummer, Aging effects of polyamide 12 in selective laser sintering: molecular weight distribution and thermal properties, Addit. Manuf. 25 (2019) 1–9, https://doi.org/10.1016/j.addma.2018.11.007.
[7] O.A. Alo, I.O. Otunniyi, D. Mauchline, Correlation of reuse extent with degradation degree of PA 12 powder during laser powder bed fusion and mechanical behavior of sintered parts, Polym. Eng. Sci. 63 (2023) 126–138, https://doi.org/10.1002/pen.26191.
[8] T. Stiller, E. Truszkiewicz, T. Schrank, B.E. Haar, G. Meier, W. Kraschitzer, G. Pinter, J. Lackner, M. Berer, Polyamide 12 powder ageing in laser beam-based powder bed fusion and its combined effects on powder and component characteristics, Rapid Prototyp. J. 31 (2025) 82–96, https://doi.org/10.1108/RPJ-08-2024-0351.
[9] R.D. Goodridge, R. Hague, C.J. Tuck, Effect of long-term ageing on the tensile properties of a polyamide 12 laser sintering material, Polym. Test. 29 (2010) 483–493, https://doi.org/10.1016/j.polymertesting.2010.02.009.
[10] D.T. Pham, K.D. Dotchev, W.A.Y. Yusoff, Deterioration of polyamide powder properties in the laser sintering process, Proc. Inst. Mech. Eng. C: J. Mech. Eng. Sci. 222 (2008) 2163–2176, https://doi.org/10.1243/09544062JMES839.
[11] P. Chen, M. Tang, W. Zhu, L. Yang, S. Wen, C. Yan, Z. Ji, H. Nan, Y. Shi, Systematical mechanism of polyamide-12 aging and its micro-structural evolution during laser sintering, Polym. Test. 67 (2018) 370–379, https://doi.org/10.1016/j.polymertesting.2018.03.035.
[12] A. Gazzerro, W. Polini, L. Sorrentino, G. Giuliano, Aging of PA12 powder in powder bed fusion, Appl. Sci. 13 (2023) 5599, https://doi.org/10.3390/app13095599.
[13] A. Wegner, C. Mielicki, T. Grimm, B. Gronhoff, G. Witt, J. Wortberg, Determination of robust material qualities and processing conditions for laser sintering of polyamide 12, Polym. Eng. Sci. 54 (2014) 1540–1554, https://doi.org/10.1002/pen.23696.
[14] B. Yao, Z. Li, F. Zhu, Effect of powder recycling on anisotropic tensile properties of selective laser sintered PA2200 polyamide, Eur. Polym. J. 141 (2020) 110093, https://doi.org/10.1016/j.eurpolymj.2020.110093.
[15] R.D. Goodridge, C.J. Tuck, R. Hague, Laser sintering of polyamides and other polymers, Prog. Mater. Sci. 57 (2012) 229–267, https://doi.org/10.1016/j.pmatsci.2011.04.001.
[16] EOS GmbH, Material data sheet PA 2200. https://www.eos.info/polymer-solutions/polymer-materials/data-sheets/mds-pa-2200, 2026 accessed 7 May 2026.
[17] K. Wudy, D. Drummer, F. Kühnlein, M. Drexler, in: Influence of Degradation Behavior of Polyamide 12 Powders in Laser Sintering Process on Produced Parts, in: Proceedings of PPS-29, American Institute of Physics, Nuremberg, Germany, 2014, pp. 691–695.
[18] F. Tischer, S. Cholewa, B. Düsenberg, D. Drummer, A. Bück, W. Peukert, J. Schmidt, Closed loop recycling approach for aged polyamide 12 feedstocks for powder bed fusion by precipitation from a moderate solvent combined with solvolysis, Addit. Manuf. 107 (2025) 104822, https://doi.org/10.1016/j.addma.2025.104822.
[19] P. Gruber, B. Kryszak, M. Olejarczyk, Radiation spheroidization as a potential method enabling recycling of polyamide 12 waste from powder bed fusion of

polymers, Mater. Des. 257 (2025) 114540, https://doi.org/10.1016/j.matdes.2025.114540.
[20] R. Kobayashi, T. Kigure, Y. Yamauchi, Support-free low-temperature laser-based powder bed fusion of polymers using a semi-sintering process, Polym. (Basel) (2024) 16, https://doi.org/10.3390/polym16233278.
[21] R. Kobayashi, T. Kigure, M. Yang, Novel process for suppressing orange peel formation in polymer laser sintering through pretreatment with low-power laser irradiation, RPJ 28 (2022) 505–513, https://doi.org/10.1108/RPJ-03-2021-0068.
[22] S. Josupeit, S. Tutzschky, M. Gessler, H.-J. Schmid, Powder ageing and material properties of laser sintered polyamide 12 using low refresh rates, in: G. Witt, A. Wegner, J. Sehrt (Eds.), Neue Entwicklungen in der Additiven Fertigung, Springer Berlin Heidelberg, Berlin, Heidelberg, 2015, pp. 63–78.
[23] S. Josupeit, On the influence of thermal histories within part cakes on the polymer laser sintering process. Doctoral dissertation, Shaker Verlag GmbH, Paderborn, 2019.
[24] I. Kletetzka, R. Gawlikowicz, H.-J. Schmid, Effects of spherical fillers on the processability and mechanical properties of PA613 and PP-based LS dry blends, in: Proceedings of the 33rd Annual International Solid Freeform Fabrication Symposium, Austin, USA, 2022.
[25] P. Roumeliotis, S. Schlicht, R. Detsch, Q. Nawaz, A.R. Boccaccini, D. Drummer, Powder aging effects on mechanical and fire properties of a flame retardant PA12 in laser powder bed fusion, Polym. Test. 153 (2025) 109048, https://doi.org/10.1016/j.polymertesting.2025.109048.
[26] F. Neitzel, I. Kletetzka, H.-J. Schmid, Halogen-free flame-retardant powder materials for laser sintering evaluation and process stability analysis, in: Proceedings of the 34th Annual International Solid Freeform Fabrication Symposium, Austin, Texas, USA, thirty-fourth ed, 2023, pp. 112–130.
[27] C. Poisson, M. Colaers, P. van Puyvelde, B. Goderis, Memory effects in the quiescent crystallization of polyamide 12: self-seeding, post-condensation, disentangling, and self-nucleation beyond the equilibrium melting temperature, Macromolecules 56 (2023) 2747–2760, https://doi.org/10.1021/acs.macromol.2c02102.
[28] S. Leupold, M. Willeke, C. Leong, N. Stratmann, A. Sommereyns, A.R. Ziefuß, S.-P. Kopp, S. Barcikowski, M. Schmidt, Correlation of optical energy onto nano-additivated CuS/PA12 and LaB6/PA12 powder with depth of fusion in PBF-LB/P, Procedia CIRP. 124 (2024) 61–64, https://doi.org/10.1016/j.procir.2024.08.071.
[29] Evonik Operations GmbH, Product information INFINAM PA 6002 P. https://www.evonik.com/en/products/hp/pr_52049756.html, 2023 accessed 11 February 2026.
[30] C.A. Chatham, Crystallization-coalescence relationships in laser powder bed fusion: moving beyond the “sintering window, Addit. Manuf. 100 (2025) 104668, https://doi.org/10.1016/j.addma.2025.104668.
[31] B. Sanders, E. Cant, M. Jenkins, Re-use of polyamide-12 in powder bed fusion and its effect on process-relevant powder characteristics and final part properties, Addit. Manuf. 80 (2024) 103961, https://doi.org/10.1016/j.addma.2024.103961.
[32] S. Rüsenberg, Prozessqualifizierung zur verlässlichen Herstellung von Produkten im Polymer Lasersinterverfahren. Doctoral dissertation, Shaker Verlag GmbH, Paderborn, 2015.
[33] R. Seltzer, F.M. de La Escalera, J. Segurado, Effect of water conditioning on the fracture behavior of PA12 composites processed by selective laser sintering, Mater. Sci. Eng.: A 528 (2011) 6927–6933, https://doi.org/10.1016/j.msea.2011.05.045.